2021 IEEE Applied Power Electronics Conference and Exposition (APEC) | 978-1-7281-8949-9/21/$31.00 ©2021 IEEE | DOI: 10.1109/APEC42165.2021.9487405

Inductor and Transformer-Coupled Magnetic Structure for Zero-Ripple dc-dc Ćuk Converter

David Porras Fernandez*, Roberto A. Fantino†, Juan C. Balda‡, Sudip K. Mazumder§

*†‡*Department of Electrical Engineering, University of Arkansas, Fayetteville, USA*

§*Department of Electrical and Computer Engineering, University of Illinois Chicago, Chicago, USA*

(e-mails: *daporras@uark.edu; †rafantin@uark.edu; ‡jbalda@uark.edu,§sudipkumarmazumder@gmail.com)

***Abstract*—An inductor and transformer-coupled integrated magnetics (IM) structure is proposed to achieve zero inductor current ripple in a dc-dc isolated Ćuk converter. The structure provides an easy-to-build approach, overcoming the necessity of a cumbersome trade-off calibration for the air gaps and number of turns, as required in the conventional IM approach used for the Ćuk dc-dc topology. The validity and effectiveness of the proposed magnetic structure is demonstrated by simulation and experimental results on dc-dc isolated Ćuk converter prototype.**

***Index Terms*—dc-dc converter, integrated magnetics, isolated Ćuk converter, zero ripple.**

I. Introduction

THE dc-dc Ćuk converter proposed in [1] has been analyzed and studied thoroughly for several different applications, configurations and topology modifications. [2]–[10]. This converter uses the least number of storage and switching elements in comparison to other dc-dc converters topologies. The advantages of this topology include low number of components, operation with low voltage ripple and low current ripple in both input and output, and output voltages greater than or less than the input voltages [11]–[13].

After the invention of the Ćuk converter, the concept of coupling inductances in switching converters grew more popular. This paved the way for the investigation of integrated-magnetics (IM) structures that promise a further reduction in size, weight, and magnetic losses [1], [11], [14], [15]. With this, the topology can be adapted for applications requiring input/output galvanic isolation [5], [16]–[18].

The IM topology proposed in [11], where the transformer and inductors are built in the same magnetic structure (MS), allows one to obtain zero current ripple in both the input and output currents of the dc-dc Ćuk converter. However, a cumbersome fine-tuning of the IM air gap and number of turns of its windings is required to satisfy the ripple-cancellation condition [11]; an important reason on why this topology is not extensively used in practical applications [14], [15], [19].

In this work, a simpler IM structure, which is easier to build and calibrate to achieve the ripple cancellation, is outlined. The validity and effectiveness of the proposed IM structure is demonstrated by both simulation and experimental results using a 1-kW dc-dc converter prototype.

This paper is organized as follows. Section II describes the isolated dc-dc Ćuk converter topology with the MS. Section III describes the MS proposed by Ćuk in [11]. Section IV describes the MS proposed in this work. In section V and VI simulation and experimental results are presented, respectively.

II. Isolated DC-DC Ćuk Converter Topology

Fig. 1 shows the circuit of the considered isolated dc-dc Ćuk converter topology allowing for bidirectional power flow; if it is not required, a single diode can be used instead of the active switch S_2. The switches S_1 and S_2 work in a complementary way. That is, when S_1 is on and S_2 is off, the voltage source V_{in} in supplies energy to the inductor L_1 while the capacitors C_a and C_b discharge energy into the inductor L_2, the filter capacitor C_{out} and the resistive load R_L. Alternatively, when S_1 is off and S_2 is on, the energy of the inductor L_1 charges the capacitors C_a and C_b, while L_2 transfers its energy to C_{out} and R_L keeping a continuous power flow to the load. The block MS (magnetic structure) in Fig. 1 comprises the inductors L_1, L_2, and a transformer T_1 with n turn ratio. In the next sections, two alternatives to implement MS are addressed, while the remaining components of the circuit in Fig. 1 are not modified.

III. Ćuk MS

Fig. 2a illustrates the structure of the IM transformer proposed in [11], and Fig. 2b shows its equivalent electric circuit representation, this structure represents an alternative to implement the MC block shown in Fig. 2. This structure, [11] is obtained by integrating the inductors L_1 and L_2 in the same magnetic structure as the transformer by using the outer legs of the core to place the inductors windings as is shown in Fig. 2a. The inductors in this magnetic structure are coupled with the transformer, but the inductors are not directly coupled between them. The coupling coefficients are given by [11]:

$$k_1 = \frac{L_M}{2\sqrt{(L_p + L_M) \cdot L_M}} \tag{1}$$

$$k_2 = \frac{L_M}{2\sqrt{(L_s + L_M) \cdot L_M}} \tag{2}$$

where L_p and L_s are the non-coupled parts of L_1 and L_2, respectively, and the non-coupled parts of the transformer (leakage inductances) are neglected. To achieve the zero-ripple

Authorized licensed use limited to: Sudip Mazumder. Downloaded on December 28,2021 at 17:09:55 UTC from IEEE Xplore. Restrictions apply.

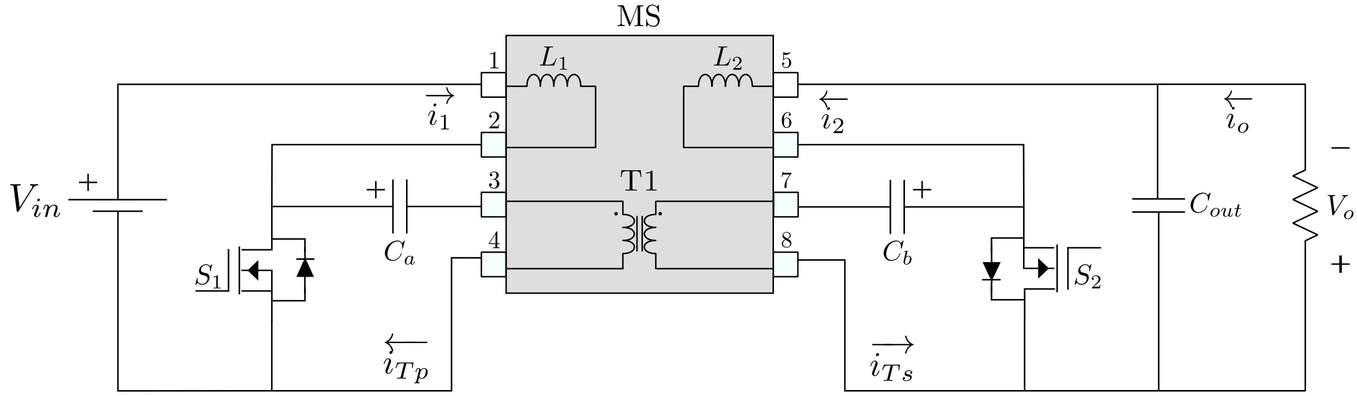

Fig. 1: Basic isolated Ćuk converter topology.

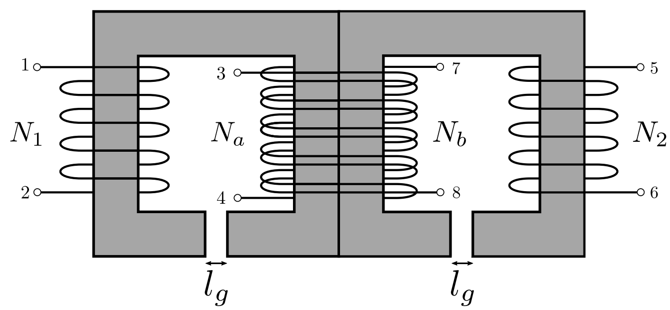

(a)

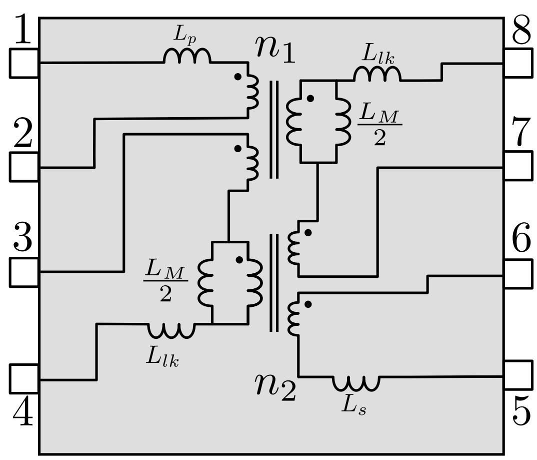

(b)

Fig. 2: Ćuk IM [11]: (a) MS. (b) Equivalent circuit.

cancellation condition in the currents i_1 and i_2 (see Fig. 1), the conditions $n_1 = 1/k_1$ and $n_2 = k_2$ must be satisfied, that is [11]:

$$n_1 = \sqrt{\frac{2 \cdot L_1}{L_M}} \tag{3}$$

$$n_2 = \sqrt{\frac{L_M}{2 \cdot L_2}} \tag{4}$$

The equivalent turns ratios n_1 and n_2 are not equal to the windings turns ratio N_1/N_a and N_2/N_b (see Fig. 2) because of the presence of L_p and L_s (non-coupled parts of the inductors). This means that in practice, a cumbersome empirical calibration of the air gaps [l_g in Fig. 2(a)] and the number of turns of the IM windings are required to achieve the condition in 3 and 4 [11], [15], [20].

The other requirement to meet, as is stated in [11]:

"Any given switching converter, with a number of separate inductors, can be integrated into a single magnetic structure provided the inductor voltages waveforms are in a fixed ratio of proportionality to one another".

This implies that to achieve the ripple cancellation with the structure in Fig. 2, the voltage waveform applied to the transformer windings should be the same as the voltage applied across the corresponding coupled inductors. To make this possible, the voltage across the series capacitors C_a and C_b should be $V_{Ca} = V_{in}$ and $V_{Cb} = V_{out}$ (see Fig. 1). This condition would be almost impossible to meet because of the ripple content on the series capacitors C_a and C_b [15].

IV. PROPOSED MS

Fig. 3 illustrates the proposed MS consisting of four-windings wounded around the center leg of the same core as is shown in Fig. 3a. The equivalent electric circuit representation of this structure is shown in Fig. 3b. The four-windings are coupled and designed to have low leakage inductances L_{lkp}, L_{lks} and L_{lkT} [see Fig. 3b], that is, $k_1 \approx 1$ and $k_2 \approx 1$. The number of turns are built under the condition $N_1 = N_a$ and $N_2 = N_b$, then the conditions to achieve the ripple cancellation are satisfied, i.e.:

$$n_1 = \frac{N_1}{N_a} = 1 \approx \frac{1}{k_1}, \tag{5}$$

$$n_2 = \frac{N_2}{N_b} = 1 \approx k_2. \tag{6}$$

As long as (5) and (6) are satisfied, the transformer can be built with any arbitrary turn ratio N_a/N_b. Regarding the

Authorized licensed use limited to: Sudip Mazumder. Downloaded on December 28,2021 at 17:09:55 UTC from IEEE Xplore. Restrictions apply.

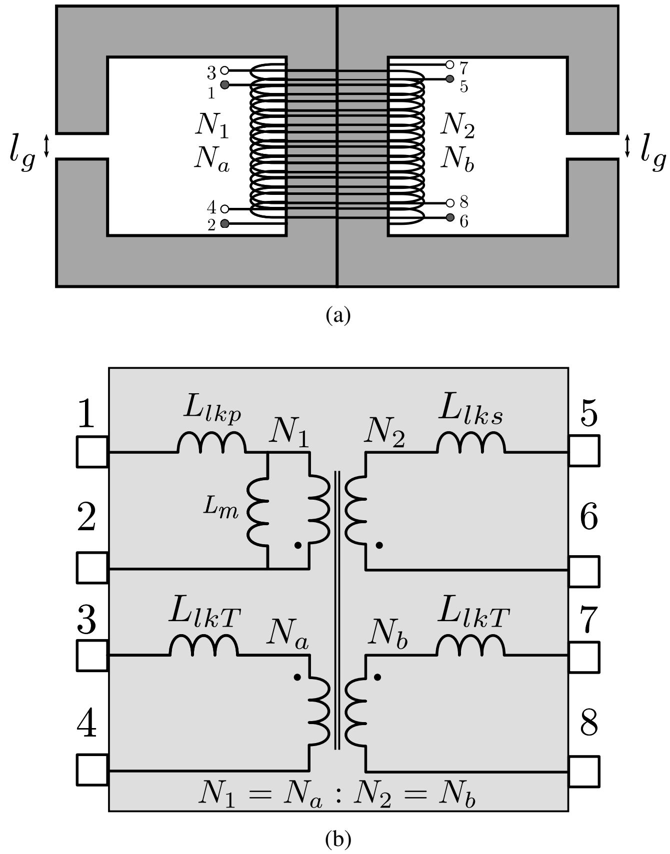

Fig. 3: Proposed IM: (a) MS. (b) Equivalent circuit.

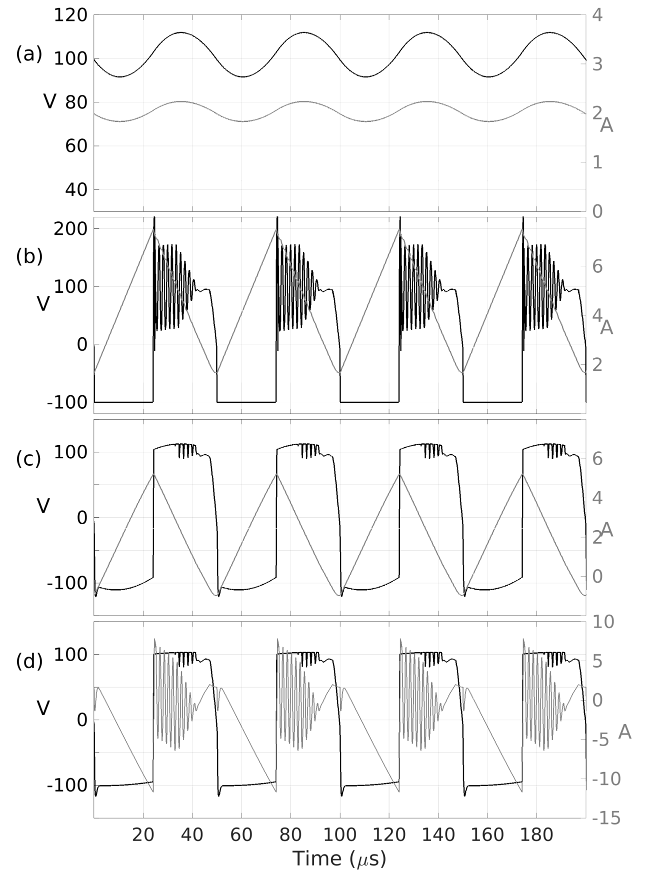

Fig. 4: Simulation, uncoupled MC: (a) V_{out} and i_{out}. (b) V_{Ls} and i_1. (c) V_{Ls} and i_2. (d) V_{T1} and i_{T1} .

second condition $V_{Ca} = V_{in}$ and $V_{Cb} = V_{out}$, note that if this condition is not satisfied the difference $(V_{Ca} - V_{in})$ is applied to the leakage inductance L_{lkp} producing a ripple in the current i_1, and the difference $(V_{Cb} - V_{out})$ is applied to the leakage inductance L_{lks} producing ripple in the current i_2. This issue can be easily overcome, with an adequate selection of the values of the capacitors C_a and C_b to minimize $(V_{Ca} - V_{in})$ and $(V_{Cb} - V_{out})$ and by increasing the values of L_{lkp} and L_{lks} by adding small series external inductors [21]. Thus, the construction process of the outlined MS is simplified with respect to the MS in Fig. 2 because there is no need to do any fine-tuning on the air gaps or turn ratio.

V. Simulation Results of the IM Structure

The system in Fig. 1 was simulated to analyze its behavior and compare the different MS. The parameters used for the system are listed in Table I. Fig. 4 displays the results of the simulations for the circuit in Fig. 1, with the inductors and transformer decoupled. An adequate snubber circuit was added to the switches to limit the overshoot voltage. In order to compare it with the proposed MS approach in Fig. 1, the inductors L_1 and L_2 consists of the sum of the inductances L_p and L_M, this makes the size of the inductors for all the three circuits the same. Fig. 4(a) displays V_{out} (in black) and the output current (in gray). Figs. 4(b) and 4(c) show the voltage across and current through the inductors; it is observed that both the currents have high ripple contents.

Fig. 5 presents the voltage and current across the inductors for the MS shown in Fig. 3 for a transformer with turns ratio $N_a/N_b = 1$. Comparing the results in Figs. 4 and 5, a tangible reduction in the ripple currents is evident for the MS depicted in Fig. 3. To demonstrate that the proposed MS is valid for any transformer turn ratio, Fig. 6 shows the same simulation results as in Fig. 5, but for the case $N_a/N_b = 2$. This shows that the ripple cancellation can be achieved for any value of N_a/N_b as long as the conditions (5) and (6) are satisfied.

VI. Experimental Results of the IM Structure

A scaled-down prototype IM-based dc-dc converter was built to test the effectiveness of the proposal. Fig. 7a shows the experimental setup used for the implementation, and Fig. 7b shows the implemented MS. A PWM signal with a duty cycle of 0.5 was implemented on a DSP (TMS320F2837xD). The parameters used for the prototype are listed on Table I. Fig. 8 shows the same voltages and currents given in Fig. 5 for the experimental implementation of the system in Fig. 1

Authorized licensed use limited to: Sudip Mazumder. Downloaded on December 28,2021 at 17:09:55 UTC from IEEE Xplore. Restrictions apply.

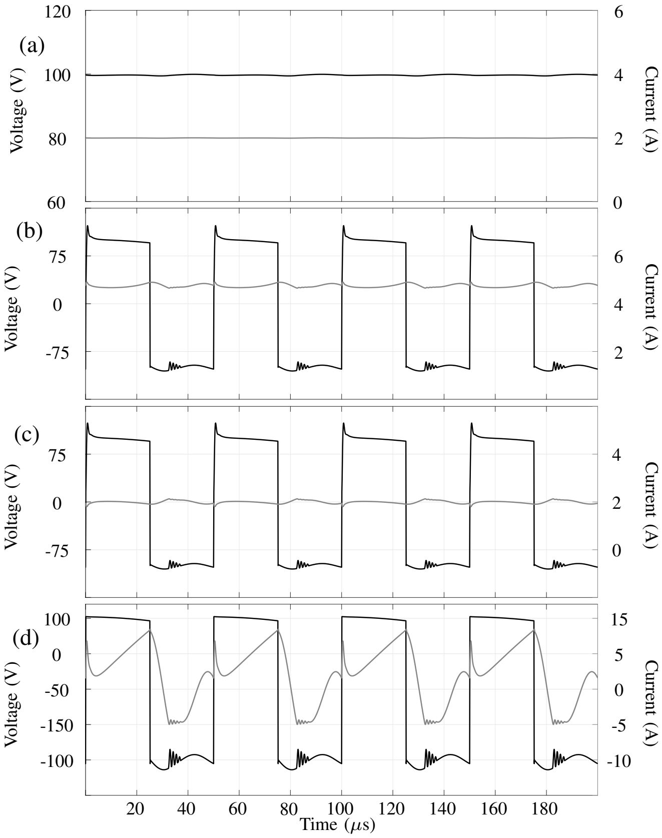

Fig. 5: Simulation results for the proposed IM: (a) V_{out} and i_{out}. (b) V_{Ls} and i_1. (c) V_{Ls} and i_2. (d) V_{T1} and i_{T1}.

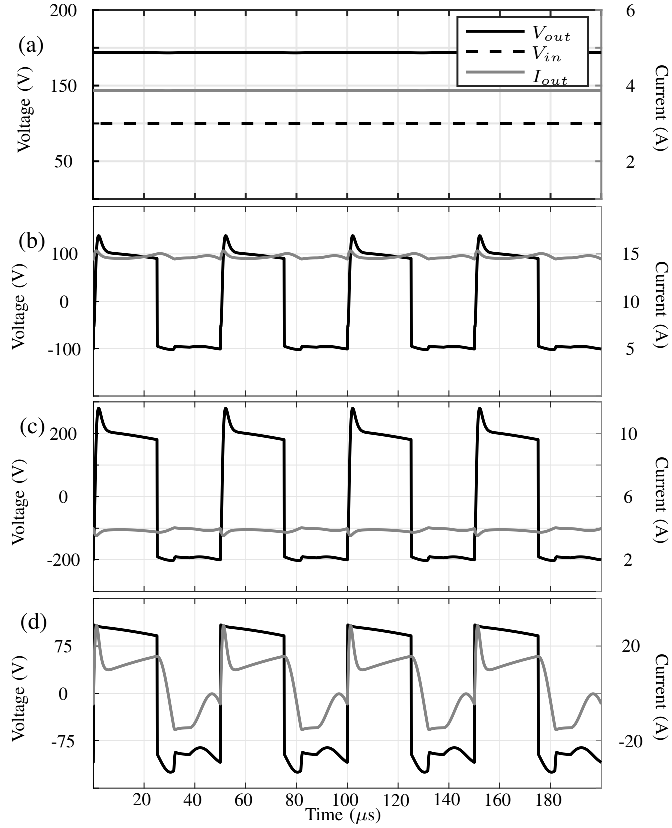

Fig. 6: Simulation results for the proposed IM with a 2 to 1 ratio: (a) V_{out} and i_{out}. (b) V_{Ls} and i_1. (c) V_{Ls} and i_2. (d) V_{T1} and i_{T1}.

when the MC block is implemented by using the proposed IM in Fig. 3. Fig. 8(a) illustrates the output voltage and current. Figs. 8(b) and 8(c) present the voltages and currents on the inductors L_1 and L_2. Fig. 8(d) displays the voltage and current on the primary winding of the transformer. Notice that when compared to the simulation data in Fig. 5, the waveforms are within the expected results.

VII. CONCLUSIONS

An inductor and transformer-coupled magnetic structure was outlined achieving zero inductor current ripple in a dc-dc isolated Ćuk converter. The structure provides a simpler design and building process with similar results regarding inductor ripple cancellation as the conventional integrated-magnetic transformer structure. A theoretical overview of the proposed integrated-magnetic structure and design was performed to compare it with conventional approach. Simulation and experimental results verified the effectiveness of the proposed structure.

TABLE I: System Parameters

Symbol	Value	Symbol	Value
V_{in}	$100\,V$	V_{out}	$100\,V$ / $200\,V$
L_1	$L_p + L_M$	L_2	$L_s + L_M$
L_p	$125\,\mu H$	L_s	$125\,\mu H$
C_a	$15\,\mu F$	C_b	$15\,\mu F$
C_{in}	$3\,\mu F$	C_{out}	$3\,\mu F$
L_M	$285\,\mu H$	R_L	$50\,\Omega$

ACKNOWLEDGMENT

This material is based upon work supported by the Department of Energy under Award Number DE-OE0000909, awarded to NextWatt LLC in 2019. The work outlined in this manuscript is encompassed in part by the following IP: S.K. Mazumder, Solid-State Power-Conversion System, Application No.62/953,465, Filing Date: December 24, 2019.

REFERENCES

[1] S. Cuk and R. Middlebrook, “A new optimum topology switching dc-to-dc converter,” in *1977 IEEE Power Electronics Specialists Conference*. IEEE, 1977, pp. 160–179.

[2] H. Zhong, J. Li, and Y.-X. Wang, “A bus-based battery equalization via modified isolated cuk converter governed by adaptive control,” in *2019 Chinese Automation Congress (CAC)*. IEEE, 2019, pp. 2824–2828.

[3] M. M. Rahman, M. N. Uddin, and M. K. Islam, “Performance enhancement of a bi-directional dc-dc converter using a ćuk converter for electric vehicle applications,” in *2015 IEEE 28th Canadian Conference on Electrical and Computer Engineering (CCECE)*. IEEE, 2015, pp. 875–880.

Authorized licensed use limited to: Sudip Mazumder. Downloaded on December 28,2021 at 17:09:55 UTC from IEEE Xplore. Restrictions apply.

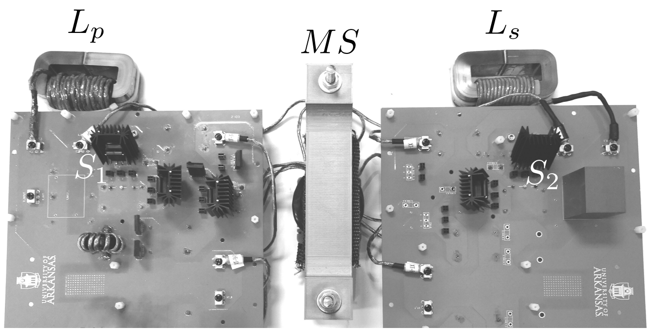

(a)

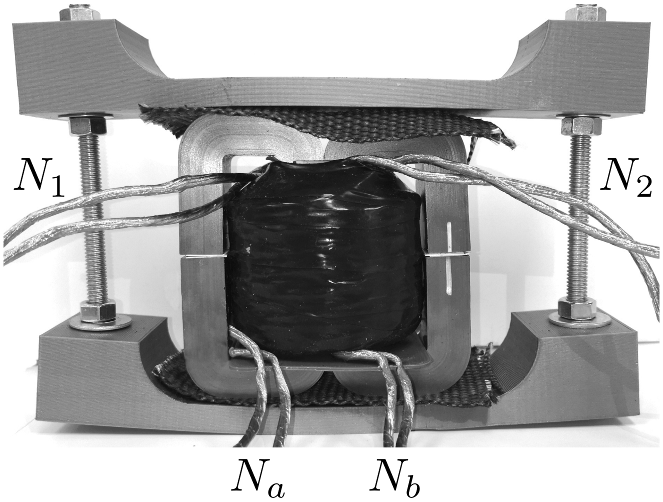

(b)

Fig. 7: Experimental setup: (a) Ćuk converter prototype (b) Proposed MS.

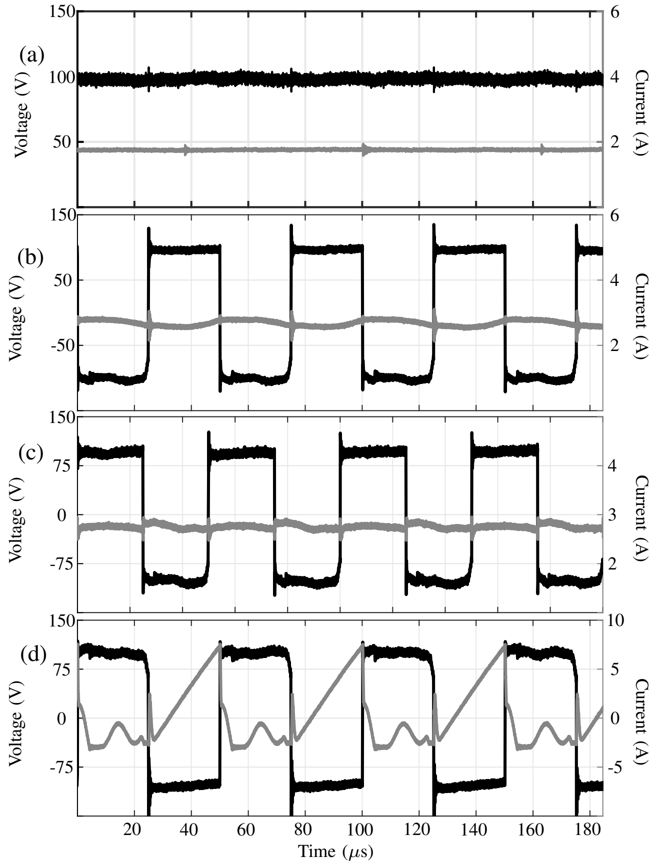

Fig. 8: Experimental results for the proposed IM: (a) V_{out} and i_{out}. (b) V_{Ls} and i_1. (c) V_{Ls} and i_2. (d) V_{T1} and i_{T1}.

[4] V. F. Pires, A. Cordeiro, D. Foito, and J. F. Silva, "High step-up dc–dc converter for fuel cell vehicles based on merged quadratic boost–ćuk," *IEEE Transactions on Vehicular Technology*, vol. 68, no. 8, pp. 7521–7530, 2019.

[5] R. Ling, Q. Dan, L. Wang, and D. Li, "Energy bus-based equalization scheme with bi-directional isolated cuk equalizer for series connected battery strings," in *2015 IEEE Applied Power Electronics Conference and Exposition (APEC)*. IEEE, 2015, pp. 3335–3340.

[6] H. Soni, S. K. Mazumder, A. Gupta, D. Chatterjee, and A. Kulkarni, "Control of isolated differential-mode single-and three-phase ćuk inverters at module level," *IEEE Transactions on Power Electronics*, vol. 33, no. 10, pp. 8872–8886, 2017.

[7] S. Mehrnami, S. K. Mazumder, and H. Soni, "Modulation scheme for three-phase differential-mode ćuk inverter," *IEEE transactions on Power Electronics*, vol. 31, no. 3, pp. 2654–2668, 2015.

[8] P. K. Maroti, S. Padmanaban, P. Wheeler, F. Blaabjerg, and M. Rivera, "Modified high voltage conversion inverting cuk dc-dc converter for renewable energy application," in *2017 IEEE Southern Power Electronics Conference (SPEC)*. IEEE, 2017, pp. 1–5.

[9] A. Kulkarni, A. Gupta, and S. K. Mazumder, "Resolving practical design issues in a single-phase grid-connected gan-fet-based differential-mode inverter," *IEEE Transactions on Power Electronics*, vol. 33, no. 5, pp. 3734–3751, 2017.

[10] N. Kumar, M. Mohamadi, and S. K. Mazumder, "Passive damping optimization of the integrated-magnetics-based differential-mode ćuk rectifier," *IEEE Transactions on Power Electronics*, vol. 35, no. 10, pp. 10 008–10 012, 2020.

[11] S. Cuk, "A new zero-ripple switching dc-to-dc converter and integrated magnetics," *IEEE Transactions on Magnetics*, vol. 19, no. 2, pp. 57–75, 1983.

[12] L. Kathi, A. Ayachit, D. K. Saini, A. Chadha, and M. K. Kazimierczuk, "Open-loop small-signal modeling of cuk dc-dc converter in ccm by circuit-averaging technique," in *2018 IEEE Texas Power and Energy Conference (TPEC)*. IEEE, 2018, pp. 1–6.

[13] B. P. Mokal and K. Vadirajacharya, "Extensive modeling of dc-dc cuk converter operating in continuous conduction mode," in *2017 International Conference on Circuit, Power and Computing Technologies (ICCPCT)*. IEEE, 2017, pp. 1–5.

[14] S. Cuk, "Integrated magnetics versus conventional power filtering," in *INTELEC'87-The Ninth International Telecommunications Energy Conference*. IEEE, 1987, pp. 61–72.

[15] Z. Zhang, "Coupled-inductor magnetics in power electronics," Ph.D. dissertation, California Institute of Technology, 1987.

[16] S. Ikeda and F. Kurokawa, "Isolated bidirectional boost full bridge dc-dc converter for energy storage system," in *2018 20th European Conference on Power Electronics and Applications (EPE'18 ECCE Europe)*. IEEE, 2018, pp. P–1.

[17] M. Kumar, Y. N. Babu, D. Pullaguram, and S. Mishra, "A high voltage gain non-isolated modified three-port dc/dc converter based on integrated boost-cuk topology," in *2017 IEEE PES Asia-Pacific Power and Energy Engineering Conference (APPEEC)*. IEEE, 2017, pp. 1–6.

[18] A. Mehdipour and S. Farhangi, "Comparison of three isolated bi-directional dc/dc converter topologies for a backup photovoltaic application," in *2011 2nd International Conference on Electric Power and Energy Conversion Systems (EPECS)*. IEEE, 2011, pp. 1–5.

[19] Z. Zhang and S. Cuk, "A high efficiency 500 w step-up cuk converter," in *Proceedings IPEMC 2000. Third International Power Electronics and Motion Control Conference (IEEE Cat. No. 00EX435)*, vol. 2. IEEE, 2000, pp. 909–914.

Authorized licensed use limited to: Sudip Mazumder. Downloaded on December 28,2021 at 17:09:55 UTC from IEEE Xplore. Restrictions apply.

[20] S. Cuk, “New magnetic structures for switching converters,” *IEEE Transactions on Magnetics*, vol. 19, no. 2, pp. 75–83, 1983.
[21] S. K. Mazumder, R. K. Burra, and K. Acharya, “A ripple-mitigating and energy-efficient fuel cell power-conditioning system,” *IEEE Transactions on Power Electronics*, vol. 22, no. 4, pp. 1437–1452, 2007.

Authorized licensed use limited to: Sudip Mazumder. Downloaded on December 28,2021 at 17:09:55 UTC from IEEE Xplore. Restrictions apply.